



A note on the audio sound power generated by a parametric array loudspeaker

Mengtong Li,¹ Jiaxin Zhong,^{2,a)}  Yun Jing,² and Jing Lu¹ 

¹Key Laboratory of Modern Acoustics and Institute of Acoustics, Nanjing University, Nanjing 210093, China

²Graduate Program in Acoustics, The Pennsylvania State University, University Park, Pennsylvania 16802, USA

ABSTRACT:

Understanding the sound power characteristics of parametric array loudspeakers (PALs) poses a unique challenge due to the nonlinear process involved. This work addresses this issue by employing the spherical convolution directivity model to obtain the far field intensity, which is then used to calculate the sound power radiated by a PAL. The results reveal that the audio sound power is approximately proportional to the square of the audio frequency and the aperture size, while inversely proportional to the ultrasound frequency. Additionally, the conversion efficiency from ultrasound to audio sound is found to be generally below 0.15% for typical configurations.

© 2023 Acoustical Society of America. <https://doi.org/10.1121/10.0023955>

(Received 7 July 2023; revised 27 October 2023; accepted 29 November 2023; published online 20 December 2023)

[Editor: Mark F. Hamilton]

Pages: 3899–3905

I. INTRODUCTION

The parametric array loudspeaker (PAL) is an application of parametric acoustic arrays for radiating highly directional audio beams using an ultrasound carrier wave in air.¹ Although the sound field properties of PALs have been extensively investigated in existing literature,^{2,3} there remains a significant gap in our knowledge concerning the sound power, a fundamental metric for characterizing sound sources, produced by PALs. An accurate assessment of the sound power of PALs can enhance our understanding of their energy conversion characteristics. Furthermore, it is imperative to consider the sound power in some practical applications. For example, PALs have been used in active noise control systems as the control sources to minimize the radiated sound power by noise sources.^{4,5} In such scenarios, accurate analysis of the power outputs of the sources, including PALs, is essential.

The power conversion from ultrasound to audio sound is widely recognized as highly inefficient for a PAL. However, the exact level of sound power produced by the PAL remains unclear due to the intricate nature of the nonlinear process it entails. In linear acoustics, for a conventional acoustic source, electric energy is converted into mechanical vibration to emit sound waves, and the corresponding sound power is well known. However, the power conversion process is different for a PAL. In a PAL, electrical energy is converted into mechanical vibration to emit ultrasound, which is subsequently self-demodulated in air, resulting in the generation of an audio sound wave. It should be noted that the sound power of the audio sound wave is transferred from the ultrasound wave.

The audio sound produced by a PAL can be considered as radiation from an infinitely large virtual volume source, where the source density is proportional to the ultrasound field.³ Consequently, measuring the sound power becomes challenging using conventional sound power measurement methods, including those based on sound pressure, sound intensity, and vibration measurements.^{6–10} ISO 3745 provides a sound-pressure-based method to determine the sound power by measuring the sound pressure on a spherical envelope surface in the far field in an anechoic room.⁸ However, the far field of the audio sound generated by a PAL is generally located more than 10 m away from the source,² making it challenging to implement this method under practical measurement conditions as it requires a large anechoic room and accurate positioning of a huge number of measurement microphones. ISO 3741 offers a precision method based on sound pressure measurement in a reverberation chamber, where the sound power is proportional to the square of the sound pressure for locations far away from the source or chamber walls.⁷ However, the virtual audio sound source produced by a PAL tends to spread throughout the space in a reverberation chamber, making it difficult to identify a suitable measurement region far away from the source. Moreover, the direct ultrasound will interact with the reflected ultrasound and produce new virtual audio sound sources, indicating that the audio sound power is different from that measured in free field. ISO 9614 specifies sound-intensity-based methods to obtain the sound power by measuring the sound intensity on a measurement surface that either completely surrounds or hemispherically surrounds the sound source.¹⁰ However, this method is also not suitable for PALs as it is challenging to identify a suitable measurement surface, which needs to be large enough to enclose the infinite virtual source. Other measurement methods,

^{a)}Email: Jiaxin.Zhong@psu.edu

such as vibration-based measurements,^{9,11} the sound intensity scaling method using beamforming,¹² and a method based on energy density measurement in a reverberation chamber,¹³ also cannot be applied to PAL sound power measurement because of similar reasons as mentioned before. Due to the inherent difficulty of accurate measurement, theoretical prediction of the audio sound power of a PAL becomes crucial for its application and for gaining a better understanding of its radiation characteristics.

The sound power can be determined by integrating the sound intensity over an envelope enclosing the sound source, where the sound intensity is defined as the product of sound pressure and particle velocity. As the near field is complex and difficult to calculate, the envelope is typically chosen in the far field, where the sound wave can be approximated as spherical spreading with a directivity. Consequently, the sound pressure can be described in terms of directivity, while the particle velocity has only a radial component and exhibits a simple linear relationship with the sound pressure. Based on this framework, obtaining the directivity of the audio sound is the first step to calculate the sound power.

Westervelt was the first to derive the directivity for the audio sound generated by a PAL, which was then used to obtain a closed-form expression for the sound power.¹⁴ The expression shows that the audio sound power is proportional to the 4th power of the on-surface pressure amplitude, the 3rd power of audio frequency, and the 4th power of aperture size, while inversely proportional to the square of ultrasound frequency. This is found to be different from the sound power for a linear acoustic source, which is proportional to the square of the on-surface pressure amplitude, the square of the frequency, and the 4th power of the aperture size when the wavelength of sound is sufficiently larger than the aperture size, while almost independent of frequency and proportional to the square of the aperture size when the wavelength of sound is much smaller than the aperture size.

The prediction of sound power obtained by Westervelt is inaccurate as the Westervelt directivity contains significant inaccuracies. The accuracy of Westervelt directivity was then improved by Berkay and Leahy by taking into account the aperture factor and the wave shape.^{15,16} However, they are only applicable for piston sources with uniform velocity profile across the radiation surface. Gan *et al.* proposed a product directivity model in 2006, which approximates the audio sound directivity by the product of the directivity of two ultrasound waves.¹⁷ This model provides the basis for calculating the far field directivity of a PAL with an arbitrary profile, but the predicted sidelobe level was found to be much smaller than measurements. In 2015, Shi and Kajikawa proposed the convolution model, which shows better agreement with measurements and is valid for a PAL with an arbitrary profile.¹⁸ This model uses the convolution of the Westervelt directivity and ultrasound directivities to predict the audio directivity. However, the convolution model is only valid for two-dimensional radiation problems and cannot be used to calculate the sound power of PALs.

Recently, Zhong *et al.* proposed the spherical convolution model, which can be seen as an extension of the convolution model to three-dimensional problems.¹⁹ The fundamental idea is to approximate the exact ultrasound field by the inward-extrapolated far field pressure, thus, simplifying the directivity of the audio sound to a spherical convolution of the ultrasound directivity and Westervelt directivity. In addition, the aperture factor of audio sound is incorporated in this model to further improve accuracy. This model shows commendable accuracy and computational efficiency for calculating the audio sound directivity, which will be employed in this article to determine the sound power of the audio generated by a PAL. The calculated sound power is then used to examine the power conversion efficiency from the ultrasound to the audio sound. Simulations are carried out for a circular PAL with a uniform profile to explore the effects of various physical parameters.

II. THEORY

A. Calculating sound power using the directivity

The sound power of an acoustic source can be determined by integrating the sound intensity over an enveloping surface that surrounds the source. In the case of a spherical envelope and when the envelope is in the far field, this calculation is expressed as $W = \int_S I_r dS$, where S is the envelope surface, I_r represents the radial sound intensity and can be obtained using the equation $I_r = |p|^2 / (2\rho_0 c_0)$ in the far field of the sound source, p is the sound pressure, ρ_0 is the ambient density, and c_0 is the sound speed. The sound pressure in the far field can be written as $p = AD(\theta, \varphi)e^{ikr}/r$, where i is the imaginary unit, A is a constant with the unit of $\text{Pa} \cdot \text{m}$, and $D(\theta, \varphi)$ represents the far field directivity of the source. It should be noted that k represents the real part of wavenumber here, as attenuation is not considered when calculating sound power. Consequently, the sound power can be calculated as²⁰

$$W = \frac{|A|^2}{2\rho_0 c_0} \iint_{4\pi} |D(\theta, \varphi)|^2 d\Omega, \quad (1)$$

where the element of the solid angle is $d\Omega = \sin \theta d\theta d\varphi$.

To obtain the sound power of the audio sound generated by a PAL, a baffled circular PAL with a radius of a is considered in this work, which is a typical configuration in the literature as well as applications.^{3,21} The sketch of the sound power calculation for a baffled circular PAL is shown in Fig. 1. In the model, Cartesian (x, y, z) and spherical (r, θ, φ) coordinate systems are established with their origin, O , at the centroid of the PAL and the positive z axis pointing to the radiation direction, where r , θ , and φ are the radial, zenithal, and azimuthal coordinates, respectively. When the PAL radiates two harmonic ultrasound waves with frequencies f_1 and f_2 ($f_1 < f_2$), the boundary condition on the surface is $v(\mathbf{r}_s) = v_0 u_1(\mathbf{r}_s)e^{-i\omega_1 t} + v_0 u_2(\mathbf{r}_s)e^{-i\omega_2 t}$, $r_s \leq a$, where v_0 is a constant with a unit of m/s , $u_i(\mathbf{r}_s)$ is an arbitrary complex velocity profile at the source point \mathbf{r}_s , $\omega_i = 2\pi f_i$ is the

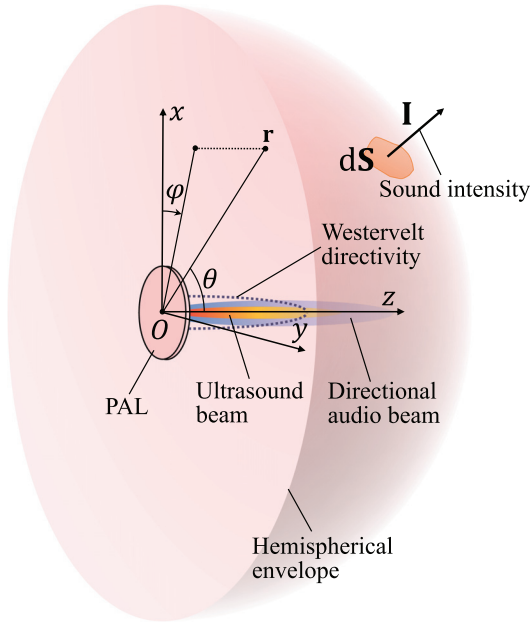


FIG. 1. (Color online) The sketch for the calculation of the sound power of a PAL.

angular frequency of the ultrasound, and the subscript $i = 1, 2$. Since the generated ultrasound pressure level is limited to ensure safety, the nonlinearity is weak, and the derivation can employ the quasilinear approximation.¹ With the successive method, the ultrasound pressure can be expressed as a twofold Rayleigh integral over the surface area of the PAL, and the audio sound pressure can be considered as a superposition of the pressure radiated by infinite virtual audio sources in air with the source density proportional to the ultrasound pressure. The audio sound pressure is then obtained by integrating the Green's function over the entire virtual source.³

The Rayleigh integral of the ultrasound pressure can be approximated in the far field as²²

$$p_i(\mathbf{r}) = \frac{p_0 \omega_i a^2}{2ic_0 r} e^{ik_i r} D_i(\theta, \varphi), \quad (2)$$

where $p_0 = \rho_0 c_0 v_0$ is the on-surface pressure amplitude, $k_i = \omega_i / c_0 + i\alpha_i$ is the complex wavenumber of the ultrasound, and α_i is the ultrasound attenuation coefficient. By substituting Eq. (2) into Eq. (1) and neglecting the imaginary part of k_i , the ultrasound power can be obtained as

$$W_i = \frac{p_0^2 \omega_i^2 a^4}{8\rho_0 c_0^3} \int_0^{2\pi} \int_0^{\pi/2} |D_i(\theta, \varphi)|^2 \sin \theta d\theta d\varphi. \quad (3)$$

Note that it integrates over a hemisphere in front of the PAL, as shown in Fig. 1, as it only radiates into half space.

The spherical convolution model¹⁹ is an accurate and computationally efficient model for calculating the far field sound pressure of PALs. The key of this model is to approximate the exact ultrasound pressure by the inward-extrapolated far field pressure given by Eq. (2), so as to

obtain the approximated virtual source density of audio sound. By substituting the approximated source density into the integral expression of audio sound field and making a far field approximation of the Green's function, the spherical convolution model predicts the far field audio sound pressure as¹⁹

$$p_a(\mathbf{r}) = -\frac{\beta p_0^2 \omega_1 \omega_2 \omega_a^2 a^4}{16\pi \alpha_t r \rho_0 c_0^6} e^{ik_a r} D_a(\theta, \varphi), \quad (4)$$

where $\alpha_t = \alpha_1 + \alpha_2$ represents the total ultrasound attenuation coefficient, and the audio sound directivity, $D_a(\theta, \varphi)$, is expressed as¹⁹

$$\begin{aligned} D_a(\theta, \varphi) &= (D_1^* D_2 \otimes D_W)(\theta, \varphi) \\ &= \int_0^{2\pi} \int_0^\pi D_1^*(\theta_v, \varphi_v) D_2(\theta_v, \varphi_v) \\ &\quad \times D_W(\gamma) \sin \theta_v d\theta_v d\varphi_v. \end{aligned} \quad (5)$$

In Eq. (5), \otimes denotes the spherical convolution operator, and γ is the angle between (θ, φ) and (θ_v, φ_v) , where $\cos \gamma = \cos \theta \cos \theta_v + \sin \theta \sin \theta_v \cos(\varphi - \varphi_v)$. D_W is the Westervelt directivity, which is defined as

$$D_W(\gamma) \equiv \frac{1}{1 - ik_a \alpha_u^{-1} \sin^2 \left(\frac{\gamma}{2} \right)}, \quad (6)$$

and $\alpha_u = (\alpha_1 + \alpha_2)/2$ represents the average ultrasound attenuation coefficient.

Equation (5) shows that the audio sound directivity is a spherical convolution of the product of ultrasound directivity $D_1^* D_2$ and the Westervelt directivity D_W . Its accuracy can be further improved by taking into account the aperture factor of audio sound to give¹⁹

$$D_a(\theta, \varphi) = D_A(\theta, \varphi) (D_1^* D_2 \otimes D_W)(\theta, \varphi), \quad (7)$$

where the effective directivity, $D_A(\theta, \varphi)$, is the far field directivity of an audio source with the same aperture size and a velocity profile of $u_a(\mathbf{r}_s) = u_1^*(\mathbf{r}_s) u_2(\mathbf{r}_s)$. In this work, the audio sound directivities obtained using Eqs. (5) and (7) are referred to as the *direct* and *modified* spherical convolution models, respectively.

By substituting Eq. (5) or Eq. (7) into Eq. (1), the audio sound power based on the spherical convolution model can be obtained as

$$W_a = \frac{\beta^2 p_0^4 a^8 \omega_1^2 \omega_2^2 \omega_a^4}{512\pi^2 \alpha_t^3 \rho_0^3 c_0^{13}} \int_0^{2\pi} \int_0^{\pi/2} |D_a(\theta, \varphi)|^2 \sin \theta d\theta d\varphi. \quad (8)$$

Equation (8) is one of the main results in this work. It follows that the audio sound power, W_a , is proportional to the 4th power of the amplitude of the ultrasound, p_0^4 . The effects of other physical parameters, such as audio sound frequency, f_a , aperture size, a , and ultrasound frequency, f_i , cannot be directly observed, as the integral term in Eq. (8) cannot be simplified to a closed-form expression.

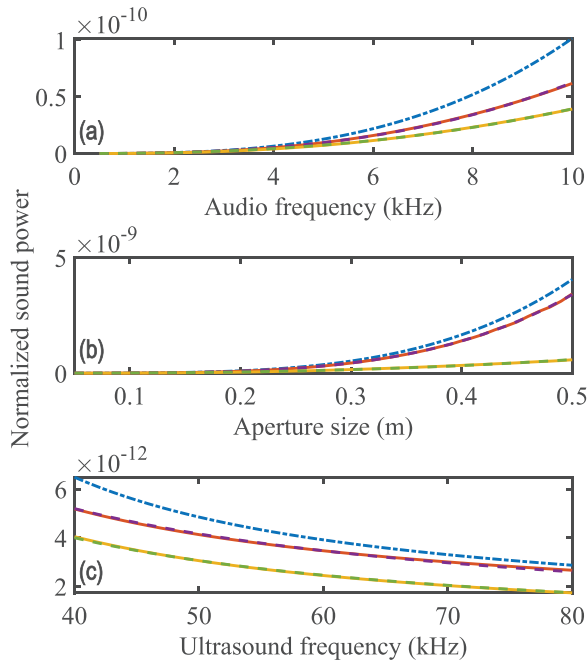


FIG. 2. (Color online) The normalized audio sound power (W/Pa^4), W_a , of a circular PAL with a uniform profile for varying (a) audio frequency, (b) aperture size, and (c) ultrasound frequency. Blue dashed-dotted line, Westervelt; red solid line, direct spherical convolution model; yellow solid line, modified spherical convolution model; dashed lines, fitting curves for spherical convolution models.

It is worth mentioning that Westervelt derived the far field audio sound pressure as $p_a(\mathbf{r}) = -\beta p_0^2 \omega_a^2 a^2 / (4\alpha_i r \rho_0 c_0^4) e^{ik_a r} D_w(\theta)$ and calculated the audio sound power using the method described by Eq. (1), providing a closed-form expression as¹⁴

$$W_{a,w} = \frac{\pi^2 \beta^2 p_0^4 a^4 \omega_a^3}{32 \alpha_i \rho_0^3 c_0^8}. \quad (9)$$

Equation (9) shows that the sound power is proportional to the 4th power of the amplitude of ultrasound, p_0^4 , the 4th power of the aperture size, a^4 , and the 3rd power of the audio sound frequency, f_a^3 , and inversely proportional to the total attenuation coefficient, α_i . Since the total attenuation coefficient is approximately proportional to the square of the ultrasound frequency when the relaxation effect is negligible, the sound power is approximately inversely proportional to the square of the ultrasound frequency, f_i^2 . Additionally, it should be noted that the sound power given by Westervelt is independent of the specific ultrasound velocity profile and the shape of PALs. In contrast, the sound power calculated using Eq. (8) remains valid regardless of the profile and shape of

the PAL, as its directivity can be accurately predicated by the spherical convolution model.

B. Sound power conversion efficiency

For a PAL, the power conversion from ultrasound to audio sound is widely recognized as highly inefficient due to the intrinsic nonlinear process. However, the exact level of power conversion efficiency remains unclear, which will be investigated in this section. To simplify the analysis, a circular piston source is considered, indicating that the velocity profile is uniform across the radiation surface, although the method presented in this article is applicable for a PAL with an arbitrary profile. In such a case, the ultrasound directivity is $D_i(\theta) = 2J_1(k_i a \sin \theta) / (k_i a \sin \theta)$, where J_1 represents the Bessel function of the first kind. Consequently, the effective directivity is $D_A = 2J_1(k_a a \sin \theta) / (k_a a \sin \theta)$. By substituting the ultrasound directivity into Eq. (3) and using the approximation $2J_1(k_i a) / (k_i a) \approx 1$ as $k_i a \gg 1$, the ultrasound power is obtained as

$$W_i \approx \frac{\pi a^2 p_0^2}{2 \rho_0 c_0}. \quad (10)$$

The conversion efficiency from ultrasound to audio sound is defined as

$$\eta = \frac{W_a}{W_1 + W_2} \times 100\%. \quad (11)$$

Therefore, the conversion efficiency of a circular PAL with a uniform profile can be obtained by substituting Eqs. (8) and (10) into Eq. (11) as

$$\eta = \frac{\beta^2 p_0^2 a^6 \omega_1^2 \omega_2^2 \omega_a^4}{512 \pi^3 \alpha_i^2 \rho_0^2 c_0^{12}} \int_0^{2\pi} \int_0^{\pi/2} |D_a(\theta, \varphi)|^2 \sin \theta d\theta d\varphi \times 100\%. \quad (12)$$

Equation (12) shows that the conversion efficiency is proportional to the square of the amplitude of the on-surface pressure, p_0^2 . However, the relationship between the conversion efficiency and other physical parameters cannot be determined directly.

In Westervelt's model,¹⁴ the ultrasound waves are assumed to be collimated planar and confined inside the aperture area $H(a - \rho)$, where $H(\cdot)$ is the Heaviside function, and $\rho = \sqrt{x^2 + y^2}$ is the polar radial coordinate. Consequently, the sound intensity is approximated by $I = |p_0|^2 / (2 \rho_0 c_0) H(a - \rho)$, and the sound power is obtained by $W_i = I \pi a^2 = \pi a^2 p_0^2 / (2 \rho_0 c_0)$. Finally, the expression for the conversion efficiency of Westervelt's model is then obtained by using Eq. (9) as

TABLE I. Fitting results for curves of the audio sound power, W_a , as a function of the audio frequency, f_a , at different aperture sizes, a , and ultrasound frequencies, f_u , based on the direct and modified spherical convolution models.

	$a = 0.1 \text{ m}$ $f_u = 40 \text{ kHz}$	$a = 0.2 \text{ m}$ $f_u = 40 \text{ kHz}$	$a = 0.4 \text{ m}$ $f_u = 40 \text{ kHz}$	$a = 0.1 \text{ m}$ $f_u = 60 \text{ kHz}$	$a = 0.1 \text{ m}$ $f_u = 80 \text{ kHz}$
Direct	$f_a^{2.7}$	$f_a^{2.7}$	$f_a^{2.7}$	$f_a^{2.8}$	$f_a^{2.8}$
Modified	$f_a^{2.4}$	$f_a^{2.2}$	$f_a^{1.9}$	$f_a^{2.5}$	$f_a^{2.4}$

TABLE II. Fitting results for curves of the audio sound power, W_a , as a function of the aperture size, a , at different audio frequencies, f_a , and ultrasound frequencies, f_u , based on the direct and modified spherical convolution models.

	$f_a = 1 \text{ kHz}$ $f_u = 40 \text{ kHz}$	$f_a = 4 \text{ kHz}$ $f_u = 40 \text{ kHz}$	$f_a = 8 \text{ kHz}$ $f_u = 40 \text{ kHz}$	$f_a = 4 \text{ kHz}$ $f_u = 60 \text{ kHz}$	$f_a = 4 \text{ kHz}$ $f_u = 80 \text{ kHz}$
Direct	a^4	a^4	a^4	a^4	$a^{3.9}$
Modified	$a^{3.2}$	$a^{2.6}$	$a^{2.3}$	$a^{2.4}$	$a^{2.3}$

$$\eta_w = \frac{\pi \beta^2 p_0^2 a^2 \omega_a^3}{32 \alpha_i \rho_0^2 c_0^7} \times 100\%. \quad (13)$$

Equation (13) illustrates that the power conversion efficiency is proportional to the square of the on-surface ultrasound amplitude, p_0^2 , the 3rd power of the audio sound frequency, f_a^3 , and the square of the aperture size, a^2 . Additionally, it is approximately inversely proportional to the square of the ultrasound frequency, f_i^2 .

III. NUMERICAL RESULTS

Numerical simulations were conducted using MATLAB R2022a to obtain the audio sound power given by Eq. (8) and the conversion efficiency given by Eq. (12) for a circular PAL with a uniform profile based on both direct and modified spherical convolution models given by Eqs. (5) and (7), respectively. The simulation results of sound power are normalized by p_0^4 , which is in the coefficient of the sound power expression Eq. (8). The results obtained by Westervelt's model given by Eqs. (9) and (13) are also presented for comparison. In simulations, the audio frequency, f_a , ranges from 500 Hz to 10 kHz; the aperture size, a , ranges from 0.05 to 0.5 m; and the average ultrasound frequency, f_u , ranges from 40 to 80 kHz. For the ablation studies, the audio frequency, the aperture size, and the average ultrasound frequency are set as 4 kHz, 0.1 m, and 40 kHz, respectively. The on-surface pressure p_0 is set to 28.3 Pa (120 dB), which is a typical value for practical applications. The sound attenuation coefficient due to atmospheric absorption is calculated according to ISO 9613-1, with a relative humidity of 50% and temperature of 25 °C.²³

A. Audio sound power

Figure 2 shows the normalized audio sound power for varying audio frequency, f_a , aperture size, a , and average ultrasound frequency, f_u . It is observed that the audio sound power increases as the audio frequency and aperture size increase, while it decreases as the ultrasound frequency increases. Compared with the results based on spherical convolution models, the predictions obtained by Westervelt overestimate the sound power for the parameters adopted here.

This discrepancy can be attributed to the inaccuracy of audio sound pressure predicted by Westervelt, which is reflected in two aspects. First, Westervelt's prediction for the on-axis sound pressure is slightly larger. Numerical calculation shows that the on-axis sound pressure predicted by Westervelt is approximately 1.06 times as large as that obtained from the direct spherical convolution model given by Eqs. (4) and (5) and approximately 1.1 times as large as that obtained from the modified spherical convolution model given by Eqs. (4) and (7). Second, but more importantly, as demonstrated in Ref. 19, the mainlobe of Westervelt directivity is normally broader, leading to an overestimation of the sound pressure in other directions. Meanwhile, it is observed that the predictions obtained from the direct spherical convolution model are also greater than those from the modified spherical convolution model. This discrepancy arises because the aperture factor of audio sound is taken into account by the modified spherical convolution model to improve the accuracy. As audio frequency f_a and the aperture size a increase, the discrepancy in predicted directivity between the two models increases, leading to a greater disparity in integration results in the sound power calculation.¹⁹

As shown by Eq. (8), it is challenging to directly determine the relationship between audio sound power and some key physical parameters in the spherical convolution model, as closed-form expression for audio sound directivity is unavailable. To address this, the least square fitting method is employed to determine the exponent of a power function in relation to audio frequency, aperture size, and ultrasound frequency. The obtained fitting results for varying audio frequency, aperture size, and ultrasound frequency are presented in Tables I, II, and III, respectively (the coefficients of the fitting results are omitted). The corresponding fitting curves are also depicted in Fig. 2. The results indicate that for the direct spherical convolution model, the audio sound power exhibits proportionality to $f_a^{2.7}$, a^4 , and f_u^{-1} . In contrast, for the modified spherical convolution model, the audio sound power demonstrates proportionality to $f_a^{2.4}$, $a^{2.6}$, and $f_u^{-1.2}$. These relationships differ from the predictions of Westervelt's sound power equation, Eq. (9), which states a direct proportionality to f_a^3 , a^4 , and f_u^{-2} .

TABLE III. Fitting results for curves of the audio sound power, W_a , as a function of the ultrasound frequency, f_u , at different audio frequencies, f_a , and aperture sizes, a , based on the direct and modified spherical convolution models.

	$f_a = 1 \text{ kHz}$ $a = 0.1 \text{ m}$	$f_a = 4 \text{ kHz}$ $a = 0.1 \text{ m}$	$f_a = 8 \text{ kHz}$ $a = 0.1 \text{ m}$	$f_a = 4 \text{ kHz}$ $a = 0.2 \text{ m}$	$f_a = 4 \text{ kHz}$ $a = 0.4 \text{ m}$
Direct	$f_u^{-1.1}$	f_u^{-1}	$f_u^{-0.8}$	f_u^{-1}	f_u^{-1}
Modified	$f_u^{-1.1}$	$f_u^{-1.2}$	$f_u^{-1.2}$	$f_u^{-1.6}$	f_u^{-2}

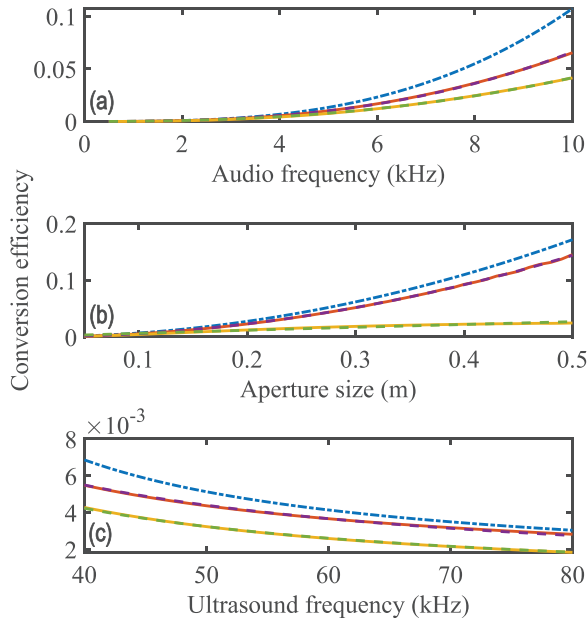


FIG. 3. (Color online) The acoustic conversion efficiency (%), η , of a circular PAL with a uniform profile for varying (a) audio frequency, (b) aperture size, and (c) ultrasound frequency. Blue dashed-dotted line, Westervelt; red solid line, direct spherical convolution model; yellow solid line, modified spherical convolution model; dashed lines, fitting curves for spherical convolution models.

Tables I–III also present the fitted expressions at some other typical values. It can be observed that for the direct spherical convolution model, the fitting exponent for audio frequency, f_a , the aperture size, a , and the ultrasound frequency, f_u , remains relatively stable across different parameter values. On the other hand, in the modified spherical convolution model, the fitting exponent for audio frequency and the ultrasound frequency decreases as the aperture size increases. Furthermore, the fitting exponent for the aperture size, a , decreases with an increase in audio frequency, f_a . This can be attributed to the dominance of the effective directivity, $D_A(\theta, \varphi)$, which is introduced in the modified spherical convolution model and primarily determined by the product of the audio frequency and the aperture size, $f_a a$. When the audio frequency and/or the aperture size increase, the mainlobe of the effective directivity becomes narrower, resulting in a reduced contribution to the overall integral.

B. Conversion efficiency

Figure 3 shows the conversion efficiency from ultrasound to audio sound, as determined by Eqs. (12) and (13), across varying audio frequency, f_a , aperture size, a , and

average ultrasound frequency, f_u . The results indicate that the overall conversion efficiency of PALs is remarkably low, with values below 0.15% for the given parameters. Westervelt's model overestimates the conversion efficiency, yielding the highest estimation, while the modified spherical convolution model gives the lowest but the most accurate prediction, which is below 0.05% for parameters adopted here. Moreover, the results reveal a consistent trend between conversion efficiency and audio sound power. Specifically, the conversion efficiency increases as the audio frequency and aperture size increase, while it decreases as the ultrasound frequency increases. This relationship can be simply deduced by examining the fitting results of the audio sound power, as the ultrasound power has a closed-form solution given by Eq. (10). Considering that the ultrasound power is independent of the audio and ultrasound frequencies, it follows the same trend of the audio sound power as shown in Tables I and III (the coefficients of the fitting results are omitted). Since the ultrasound power is proportional to the square of the aperture size, a^2 , the dependence of conversion efficiency on the aperture size can be obtained by dividing the expressions presented in Table II by a^2 , and the results are shown in Table IV (the coefficients of the fitting results are omitted).

IV. CONCLUSION

The sound power of the audio sound generated by a PAL is challenging to measure using the existing conventional sound power measurement methods. In this article, the sound power as well as the conversion efficiency from ultrasound to audio sound are calculated by integrating the far field sound intensity, which is obtained by the spherical convolution model. Since the spherical convolution model can accurately predict the directivity of the audio sound generated by a PAL, the sound power and efficiency calculated in this work are more accurate than the results obtained by Westervelt. Simulation results highlight the significantly low sound power and conversion efficiency exhibited by PALs, while also uncovering the specific relationships with several key parameters. It shows that the audio sound power is proportional to the 4th power of on-surface pressure amplitude, the 2.4th power of audio frequency, and the 2.6th power of aperture size, while inversely proportional to the 1.2th power of the ultrasound frequency. The conversion efficiency is found to be proportional to the 2nd power of ultrasound amplitude and the 0.6th power of aperture size, while the relationship with audio frequency and ultrasound frequency remains consistent with the trend of audio sound power. Despite the difficulties in direct measurement, the

TABLE IV. Fitting results for curves of the conversion efficiency, η , as a function of the aperture size, a , at different audio frequencies, f_a , and ultrasound frequencies, f_u , based on the direct and modified spherical convolution model.

	$f_u = 40 \text{ kHz}$ $f_a = 1 \text{ kHz}$	$f_u = 40 \text{ kHz}$ $f_a = 4 \text{ kHz}$	$f_u = 40 \text{ kHz}$ $f_a = 8 \text{ kHz}$	$f_u = 60 \text{ kHz}$ $f_a = 4 \text{ kHz}$	$f_u = 80 \text{ kHz}$ $f_a = 4 \text{ kHz}$
Direct	a^2	a^2	a^2	a^2	$a^{1.9}$
Modified	$a^{1.2}$	$a^{0.6}$	$a^{0.3}$	$a^{0.4}$	$a^{0.3}$

calculation method proposed in this article offers a reliable approach for predicting sound power, which may provide insights and guidance for the applications of PALs. In the future, further research will be conducted to develop appropriate methods for measuring the sound power of PALs. It is worth noting that the proposed theory relies on the assumption of the quasilinear approximation. However, in certain applications characterized by strong nonlinearity, the quasilinear approximation may not be applicable. In such cases, it becomes necessary to develop a more comprehensive theory to accurately predict the sound power generated by a PAL.

ACKNOWLEDGMENTS

This work was supported by the National Natural Science Foundation of China (Grant No. 12274221).

AUTHOR DECLARATIONS

Conflict of Interest

The authors have no conflicts of interest to disclose.

DATA AVAILABILITY

The data that support the findings of this study are available from the corresponding author upon reasonable request.

- ¹W.-S. Gan, J. Yang, and T. Kamakura, "A review of parametric acoustic array in air," *Appl. Acoust.* **73**(12), 1211–1219 (2012).
- ²J. Zhong, R. Kirby, and X. Qiu, "The near field, Westervelt far field, and inverse-law far field of the audio sound generated by parametric array loudspeakers," *J. Acoust. Soc. Am.* **149**(3), 1524–1535 (2021).
- ³J. Zhong, R. Kirby, and X. Qiu, "A spherical expansion for audio sounds generated by a circular parametric array loudspeaker," *J. Acoust. Soc. Am.* **147**(5), 3502–3510 (2020).
- ⁴C. Ye, M. Wu, and J. Yang, "Actively created quiet zones by parametric loudspeaker as control sources in the sound field," *AIP Conf. Proc.* **1474**, 367–374 (2012).
- ⁵N. Tanaka and M. Tanaka, "Mathematically trivial control of sound using a parametric beam focusing source," *J. Acoust. Soc. Am.* **129**(1), 165–172 (2011).
- ⁶ISO 3740:2019, "Acoustics—Determination of sound power levels of noise sources—Guidelines for the use of basic standards" (International Organization for Standardization, Geneva, Switzerland, 2019).

- ⁷ISO 3741:2010, "Acoustics—Determination of sound power levels and sound energy levels of noise sources using sound pressure—Precision methods for reverberation test rooms" (International Organization for Standardization, Geneva, Switzerland, 2010).
- ⁸ISO 3745:2012, "Acoustics—Determination of sound power levels and sound energy levels of noise sources using sound pressure—Precision methods for anechoic rooms and hemi-anechoic rooms" (International Organization for Standardization, Geneva, Switzerland, 2012).
- ⁹ISO/TS 7849-1:2009, "Acoustics—Determination of airborne sound power levels emitted by machinery using vibration measurement—Part 1: Survey method using a fixed radiation factor" (International Organization for Standardization, Geneva, Switzerland, 2009).
- ¹⁰ISO 9614-1:1993, "Acoustics—Determination of sound power levels of noise sources using sound intensity—Part 1: Measurement at discrete points" (International Organization for Standardization, Geneva, Switzerland, 1993).
- ¹¹T. P. Bates, I. C. Bacon, J. D. Blotter, and S. D. Sommerfeldt, "Vibration-based sound power measurements of arbitrarily curved panels," *J. Acoust. Soc. Am.* **151**(2), 1171–1179 (2022).
- ¹²J. Hald, "Estimation of partial area sound power data with beamforming," in *INTER-NOISE and NOISE-CON Congress and Conference Proceedings*, Rio de Janeiro, Brazil (August 7–10, 2005) (Institute of Noise Control Engineering – USA, Washington, DC, 2005), pp. 2424–2433.
- ¹³D. B. Nutter, T. W. Leishman, S. D. Sommerfeldt, and J. D. Blotter, "Measurement of sound power and absorption in reverberation chambers using energy density," *J. Acoust. Soc. Am.* **121**(5), 2700–2710 (2007).
- ¹⁴P. J. Westervelt, "Parametric acoustic array," *J. Acoust. Soc. Am.* **35**(4), 535–537 (1963).
- ¹⁵H. O. Berktaý, "Possible exploitation of non-linear acoustics in underwater transmitting applications," *J. Sound Vib.* **2**(4), 435–461 (1965).
- ¹⁶H. O. Berktaý and D. J. Leahy, "Farfield performance of parametric transmitters," *J. Acoust. Soc. Am.* **55**(3), 539–546 (1974).
- ¹⁷W.-S. Gan, J. Yang, K.-S. Tan, and M.-H. Er, "A digital beamsteerer for difference frequency in a parametric array," *IEEE/ACM Trans. Audio Speech Lang. Process.* **14**(3), 1018–1025 (2006).
- ¹⁸C. Shi and Y. Kajikawa, "A convolution model for computing the far-field directivity of a parametric loudspeaker array," *J. Acoust. Soc. Am.* **137**(2), 777–784 (2015).
- ¹⁹J. Zhong, H. Zou, J. Lu, and D. Zhang, "A modified convolution model for calculating the far field directivity of a parametric array loudspeaker," *J. Acoust. Soc. Am.* **153**(3), 1439–1451 (2023).
- ²⁰H. Kuttruff, *Acoustics: An Introduction* (CRC, Boca Raton, FL, 2007).
- ²¹M. Červenka and M. Bednařík, "Non-paraxial model for a parametric acoustic array," *J. Acoust. Soc. Am.* **134**(2), 933–938 (2013).
- ²²L. W. Schmerr, Jr., *Fundamentals of Ultrasonic Phased Arrays* (Springer, New York, 2014).
- ²³ISO 9613-1:1993, "Acoustics—Attenuation of sound during propagation outdoors—Part 1: Calculation of the absorption of sound by the atmosphere" (International Organization for Standardization, Geneva, Switzerland, 1993).